Atmospheric Chemistry of Trimethoxymethane, $(CH_3O)_3CH$; Laboratory Studies

J. Platz, J. Sehested,† and O. J. Nielsen*,‡

Atmospheric Chemistry, Plant Biology and Biogeochemistry Department, Risø National Laboratory, DK-4000, Roskilde, Denmark

T. J. Wallington*,§

Ford Motor Company, 20000 Rotunda Drive, Mail Drop SRL-3083, Dearborn, Michigan 48121-2053

Received: June 23, 1998; In Final Form: December 30, 1998

A pulse radiolysis technique was used to measure the UV absorption spectra of $(CH_3O)_2CHOCH_2(\cdot)$ and $(CH_3O)_2CHOCH_2O_2(\cdot)$ radicals derived from trimethoxymethane over the range 220−320 nm, $\sigma_{250\ nm}$ $(CH_3O)_2CHOCH_2(\cdot) = (2.8 \pm 0.4) \times 10^{-18}$ and $\sigma_{250\ nm}$ $(CH_3O)_2CHOCH_2O_2(\cdot) = (3.5 \pm 0.4) \times 10^{-18}$ cm^2 molecule^{-1}. The self-reaction rate constants for $(CH_3O)_2CHOCH_2(\cdot)$ and $(CH_3O)_2CHOCH_2O_2(\cdot)$ radicals, defined as $-d[(CH_3O)_2CHOCH_2(\cdot)]/dt = 2k_5[(CH_3O)_2CHOCH_2(\cdot)]^2$ and $-d[(CH_3O)_2CHOCH_2O_2(\cdot)]/dt = 2k_{6\ obs}[(CH_3O)_2CHOCH_2O_2(\cdot)]^2$ were $k_5 = (3.5 \pm 0.5) \times 10^{-11}$ and $k_{6\ obs} = (1.3 \pm 0.2) \times 10^{-11}$ cm^3 molecule^{-1} s^{-1}. Rate constants for reactions of $(CH_3O)_2CHOCH_2O_2(\cdot)$ radicals with NO and NO_2 were $k_7 = (9.0 \pm 1.2) \times 10^{-12}$ and $k_8 = (1.0 \pm 0.2) \times 10^{-11}$ cm^3 molecule^{-1} s^{-1}, respectively. Rate constants for the reaction of OH radicals and F atoms with trimethoxymethane and the reaction of $(CH_3O)_2CHOCH_2(\cdot)$ radicals with O_2 were $k_1 = (6.0 \pm 0.5) \times 10^{-12}$, $k_3 = (3.0 \pm 0.7) \times 10^{-10}$, and $k_2 = (9.2 \pm 1.5) \times 10^{-12}$ cm^3 molecule^{-1} s^{-1}, respectively. Relative rate techniques were used to measure k(Cl + trimethoxymethane) $= (1.5 \pm 0.2) \times 10^{-10}$ cm^3 molecule^{-1} s^{-1}. OH-radical-initiated oxidation of trimethoxymethane in air gives dimethyl carbonate in a molar yield of 81 ± 10%. These results are discussed with respect to the atmospheric chemistry of automotive fuel additives.

1. Introduction

There are commercial and environmental pressures on vehicle manufacturers to produce vehicles with increased fuel economy. Diesel engines operate at a greater compression ratio and have a greater thermodynamic efficiency than gasoline engines. Increased use of diesel engines is an attractive method to increase fuel economy. Unfortunately, diesel engines running on conventional fuels have a tendency to produce substantial particulate emissions. Dimethyl ether (DME) has been proposed as a possible alternative diesel fuel because it combines acceptable fuel properties (i.e., high cetane number) with low exhaust emissions (especially particulate), and low combustion noise.[1] In addition to DME, other ethers such as diethyl ether and dimethoxy methane (DMM) are undergoing testing as new diesel fuels. To predict the environmental impact of the use of ethers as diesel fuels it is desirable to understand how molecular structure impacts their atmospheric reactivity. As a part of a collaborative study of the atmospheric chemistry of alternative diesel fuels we have undertaken a study of trimethoxymethane, $(CH_3O)_3CH$, which has obvious structural similarities to DME and DMM.

The atmospheric degradation of $(CH_3O)_3CH$ will be initiated by reaction with OH radicals generating alkyl radicals which react with O_2 to give alkyl peroxy radicals:

$$(CH_3O)_3CH + OH \rightarrow (CH_3O)_2CHOCH_2(\cdot) + H_2O \quad (1a)$$

$$(CH_3O)_3CH + OH \rightarrow (CH_3O)_3C(\cdot) + H_2O \quad (1b)$$

$$(CH_3O)_2CHOCH_2(\cdot) + O_2 + M \rightarrow (CH_3O)_2CHOCH_2O_2(\cdot) + M \quad (2)$$

$$(CH_3O)_3C(\cdot) + O_2 + M \rightarrow (CH_3O)_3CO_2(\cdot) + M \quad (3)$$

We have used pulse radiolysis coupled with time-resolved UV−vis absorption spectroscopy and FTIR−smog chamber techniques to determine the UV absorption spectra of the alkyl and alkyl peroxy radicals derived from trimethoxymethane, the kinetics of reactions 1−8, and the atmospheric oxidation products of trimethoxymethane.

$$F + (CH_3O)_3CH \rightarrow \text{products} \quad (4)$$

$$(CH_3O)_2CHOCH_2(\cdot) + (CH_3O)_2CHOCH_2(\cdot) \rightarrow \text{products} \quad (5)$$

$$(CH_3O)_2CHOCH_2O_2(\cdot) + (CH_3O)_2CHOCH_2O_2(\cdot) \rightarrow \text{products} \quad (6)$$

$$(CH_3O)_2CHOCH_2O_2(\cdot) + NO \rightarrow (CH_3O)_2CHOCH_2O(\cdot) + NO_2 \quad (7a)$$

* Authors to whom correspondence should be addressed.
† Current address: Haldor Topsoe A/S, Nymoellevej 55, DK-2800 Lyngby, Denmark. E-mail: jss@topsoe.dk.
‡ E-mail: ole.john.nielsen@risoe.dk.
§ E-mail: twalling@ford.com.

10.1021/jp9827476 CCC: $18.00
Published on Web 03/26/1999

$$(CH_3O)_2CHOCH_2O_2(\cdot) + NO + M \rightarrow (CH_3O)_2CHOCH_2ONO_2 + M \quad (7b)$$

$$(CH_3O)_2CHOCH_2O_2(\cdot) + NO_2 + M \rightarrow (CH_3O)_2CHOCH_2O_2NO_2 + M \quad (8)$$

Results are reported herein and discussed with respect to the available literature.

2. Experimental Section

Two different experimental systems were used, both have been described previously.[2,3] All experiments were conducted at 296 ± 2 K. Unless otherwise stated, all uncertainties reported in this paper are two standard deviations. Standard error propagation methods were used where appropriate.

2.1 Pulse Radiolysis System. To study the reaction between OH radicals and trimethoxymethane, OH radicals were generated from H_2O by pulsed radiolysis of Ar/H_2O gas mixtures in a 1 L stainless steel reaction cell with a 30 ns pulse of 2 MeV electrons from a Febetron 705 field emission accelerator. $(CH_3O)_2CHOCH_2(\cdot)$ radicals were generated from $(CH_3O)_3CH$ by the pulsed radiolysis of $SF_6/(CH_3O)_3CH$ gas mixtures. Ar or SF_6 diluent were always in great excess and were used to generate Ar* atoms and fluorine atoms:

$$Ar \xrightarrow{2\ MeV\ e^-} Ar^* \quad (9)$$

$$Ar^* + H_2O \rightarrow OH + H + Ar \quad (10)$$

$$F + (CH_3O)_3CH \rightarrow \text{products} \quad (4)$$

The radiolysis dose was varied by insertion of stainless steel attenuators between the accelerator and the reaction cell. In this work we refer to the radiolysis dose as a fraction of the maximum dose that is achievable. The fluorine atom yield was $(3.18 \pm 0.32) \times 10^{15}$ cm^{-3} at full radiolysis dose and 1000 mbar of SF_6[4]. OH radicals were monitored using their characteristic absorption at 309.25 nm. The initial OH concentration was of the order of 5×10^{13} cm^{-3}.

The analysis light was provided by a pulsed 150 W Xenon arc lamp and was multipassed through the reaction cell using internal White cell optics to give total optical path lengths of 120 or 160 cm. After leaving the cell, the light was guided through a monochromator (operated with a spectral resolution of 1 nm) and detected by a photomultiplier (to record absorption transients) or a diode array (to record absorption spectra). All absorption transients were derived from single pulse experiments.

Reagent purities and concentrations were Ar (ultrahigh purity) 980−990 mbar; H_2O (triple distilled deionized water) 5−15 mbar; SF_6 (99.9%) 954−997 mbar; $(CH_3O)_3CH$ (>99%) 3.0−5.2 mbar; O_2 (ultrahigh purity) 1.1−20.1 mbar; CH_4 (>99%) 2.3−45.0 mbar; NO (>99.8%) 0.11−0.94 mbar; and NO_2 (>98%) 0.11−0.81 mbar. All experiments were performed at 296 K and 1000 mbar total pressure. $(CH_3O)_3CH$ was degassed by freeze−pump−thaw cycling before use, other chemicals were used as received.

Seven sets of experiments were performed. First, the rate constant for reaction of OH radicals with $(CH_3O)_3CH$ was determined using pulse radiolysis of Ar/H_2O/$(CH_3O)_3CH$ mixtures. Second, the rate constant for reaction of F atoms with $(CH_3O)_3CH$ was determined using the pulse radiolysis of $SF_6/(CH_3O)_3CH/CH_4$ mixtures. Third, the UV absorption spectra of the alkyl and alkyl peroxy radicals derived from $(CH_3O)_3$-CH were obtained using the diode array camera to capture the UV absorption following radiolysis of $SF_6/(CH_3O)_3CH$ and $SF_6/(CH_3O)_3CH/O_2$ mixtures. Fourth, the rate constants for reactions 5 and 6 were determined from the rate of decay of the absorption at 250 nm, following the radiolysis of $SF_6/(CH_3O)_3CH$ and $SF_6/(CH_3O)_3CH/O_2$ mixtures. Fifth, the rate constant for the association reaction between O_2 and the alkyl radicals derived from $(CH_3O)_3CH$ was measured by monitoring the loss of alkyl radicals in the presence of O_2. Sixth, the rate of NO_2 formation following radiolysis of $SF_6/(CH_3O)_3CH/O_2/NO$ mixtures was monitored to measure k_7. Finally, k_8 was determined by monitoring the rate of NO_2 loss following radiolysis of $SF_6/(CH_3O)_3CH/O_2/NO_2$ mixtures.

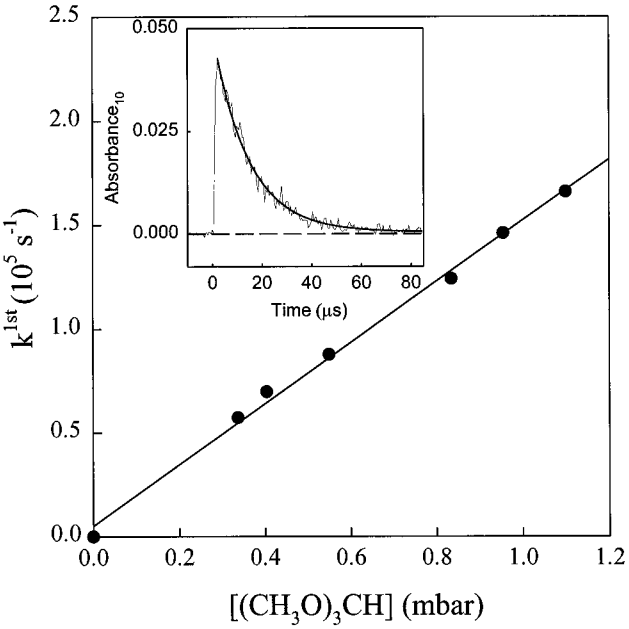

Figure 1. Pseudo-first-order loss of OH radicals versus $[(CH_3O)_3CH]$. The insert shows the transient absorbance at 309.25 nm observed following pulsed radiolysis (full dose) of a mixture containing 0.404 mbar $(CH_3O)_3CH$, 13.6 mbar H_2O, and 986 mbar Ar.

2.2 FTIR−Smog Chamber System. FTIR−smog chamber techniques were used to study the kinetics of the reaction of Cl atoms with trimethoxymethane, the atmospheric fate of the alkoxy radical derived from $(CH_3O)_3CH$, and the atmospheric oxidation products of trimethoxymethane. Experiments were conducted using a 140 L Pyrex reaction chamber[3] interfaced to an FTIR spectrometer for in situ chemical analysis. Radicals were generated by UV irradiation (22 blacklamps) of mixtures containing 7−15 mTorr of trimethoxymethane, 50−120 mTorr of Cl_2 or 100 mTorr of CH_3ONO, and 115−147 Torr of O_2 in 700 Torr total pressure using N_2 diluent at (760 Torr = 1013 mbar = 101.3 kPa). Reactant loss and product formation were monitored by FTIR spectroscopy over the wavenumber range 800−2000 cm^{-1}. The analyzing path length for the FTIR system was 28 m, the spectral resolution was 0.25 cm^{-1}. Infrared spectra were derived from 32 co-added spectra.

3. Results

3.1. Reaction of OH Radicals with $(CH_3O)_3CH$. To measure k_1, experiments were performed using pulse radiolysis of Ar/H_2O/$(CH_3O)_3CH$ mixtures at 1000 mbar total pressure and 295 K. The insert in Figure 1 shows the transient absorption at 309.25 nm following radiolysis of a mixture of 0.404 mbar $(CH_3O)_3CH$, 13.6 mbar H_2O, and 986 mbar Ar. The rapid increase in absorption observed 0−1 μs after the radiolysis pulse

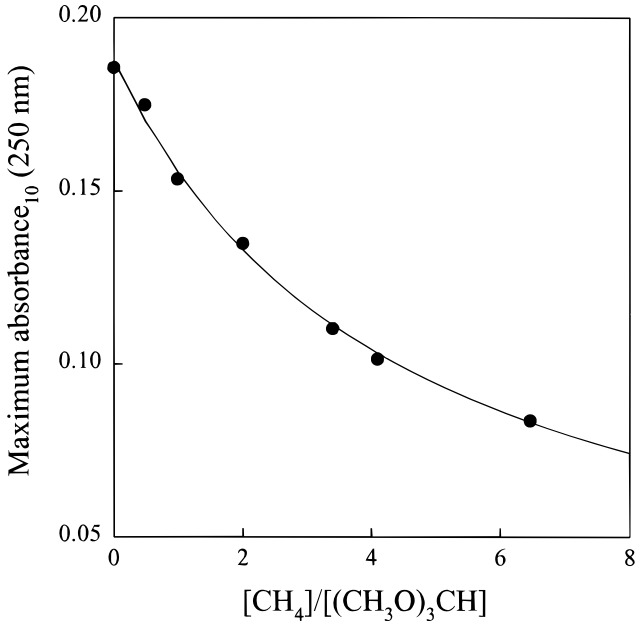

Figure 2. Maximum transient absorbance observed following radiolysis of $(CH_3O)_3CH/CH_4/SF_6$ mixtures versus the concentration ratio $[CH_4]/[(CH_3O)_3CH]$.

is attributed to the formation of OH radicals which absorb strongly at 309.25 nm. The subsequent decay of absorption followed first-order kinetics and is ascribed to loss of OH radicals via reaction with $(CH_3O)_3CH$. The smooth curve in the insert shows a fit to the data of the following expression which yields a value of $k^{first} = 7.0 \times 10^4$ s^{-1}.

$$[OH]_t = [OH]_0 \exp(-k^{first} t)$$

where $[OH]_t$ and $[OH]_0$ are the OH radical concentrations at time t and time 0 and k^{first} is the first-order rate constant of reaction 1. Figure 1 shows a plot of k^{first} versus the $(CH_3O)_3CH$ concentration. Linear least-squares regression of the data in Figure 1 gives $k_1 = (5.98 \pm 0.33) \times 10^{-12}$ cm^3 molecule^{-1} s^{-1}. To account for additional uncertainties associated with the nonlinear relationship between [OH] and the UV absorption at 309.25 nm[5] we choose to propagate an additional 5% uncertainty range and obtain a final value of $k_1 = (6.0 \pm 0.5) \times 10^{-12}$ cm^3 molecule^{-1} s^{-1}. There are no previous measurements of k_1 to compare with our result. The reactivity of OH radicals toward $(CH_3O)_3CH$ is similar to that toward DMM, $(CH_3O)_2CH_2$; k(OH + DMM) $= 5.2 \times 10^{-12}$ cm^3 molecule^{-1} s^{-1} at 295 K (average from refs 6 and 7).

3.2. Reaction of F Atoms with $(CH_3O)_3CH$. To measure k_4, the maximum transient absorbance at 250 nm was measured following the radiolysis of $SF_6/(CH_3O)_3CH/CH_4$ mixtures. The radiolysis dose (41.6% of full dose) and total pressure (1000 mbar) were held fixed. The concentrations of $(CH_3O)_3CH$ and CH_4 were varied over the ranges 0−5.2 mbar and 0−45.0 mbar, respectively. Figure 2 shows the observed maximum absorbance as a function of the concentration ratio $[CH_4]/[(CH_3O)_3CH]$. In the reaction system reactions 4 and 12 compete for the available F atoms:

$$F + (CH_3O)_3CH \rightarrow \text{products} \quad (4)$$

$$F + CH_4 \rightarrow HF + CH_3 \quad (12)$$

$(CH_3O)_2CHOCH_2(\cdot)$ radicals and $(CH_3O)_3C(\cdot)$ formed via reaction 4 absorb appreciably at 250 nm, CH_3 radicals do not. As shown in Figure 2, as the concentration ratio $[CH_4]/[(CH_3O)_3CH]$ increases, the maximum absorbance decreases because a greater fraction of the F atoms react with CH_4 to give CH_3 radicals. The solid line in Figure 2 is a three-parameter fit of the following expression to the experimental data:

$$A_{max} = (A_R + A_{CH_3}(k_{12}/k_4)\,[CH_4]/[(CH_3O)_3CH])/(1 + (k_{12}/k_4)\,[CH_4]/[(CH_3O)_3CH])$$

where A_{max} is the observed absorbance, A_R is the absorbance if only $(CH_3O)_2CHOCH_2(\cdot)$ or $(CH_3O)_3C(\cdot)$ radicals were produced, and A_{CH_3} is the absorbance if only CH_3 radicals were produced. The parameters A_R, A_{CH_3}, and k_{12}/k_4 were varied simultaneously, the best fit was obtained with $k_{12}/k_4 = (0.23 \pm 0.02)$, $A_R = (0.19 \pm 0.01)$, and $A_{CH_3} = (0.01 \pm 0.01)$. Using $k_{12} = (6.8 \pm 1.4) \times 10^{-11}$ cm^3 molecule^{-1} s^{-18} gives $k_4 = (3.0 \pm 0.7) \times 10^{-10}$ cm^3 molecule^{-1} s^{-1} which is close to the gas kinetic limit. This result is not surprising given the fact that F atoms typically react at, or close to, the gas kinetic limit with most organic compounds.[9]

3.3. Spectrum of $(CH_3O)_2CHOCH_2(\cdot)$ Alkyl Radicals. Following the pulsed radiolysis of $SF_6/(CH_3O)_3CH$ mixtures, a rapid (complete within 0.5−1 μs) increase in absorption was observed at 250 nm, followed by a slower decay. Figure 3A shows the transient absorption at 250 nm following radiolysis of a mixture of 995 mbar SF_6 and 5 mbar $(CH_3O)_3CH$. No absorption was observed when either 995 mbar SF_6 or 5 mbar $(CH_3O)_3CH$ was radiolyzed separately. We ascribe the absorption shown in Figure 3A to the formation of $(CH_3O)_2CHOCH_2(\cdot)$ alkyl radicals and their subsequent loss by self-reaction. We assume that F atoms react with $(CH_3O)_3CH$ to give $(CH_3O)_2CHOCH_2(\cdot)$ alkyl radicals. The validity of this assumption is discussed at the end of this section. To work under conditions where a known fraction of the F atoms are converted into $(CH_3O)_2CHOCH_2(\cdot)$ radicals, it is necessary to consider potential interfering radical−radical reactions such as (5) and (13):

$$(CH_3O)_2CHOCH_2(\cdot) + (CH_3O)_2CHOCH_2(\cdot) \rightarrow \text{products} \quad (5)$$

$$F + (CH_3O)_2CHOCH_2(\cdot) \rightarrow \text{products} \quad (13)$$

To check for such complications, experiments were performed using mixtures of 995 mbar of SF_6 and 5 mbar of $(CH_3O)_3CH$, with the maximum transient absorption at 250 nm measured as a function of radiolysis dose. Figure 4A shows the observed maximum absorbance from experimental transients ascribed to alkyl radicals as a function of the dose. As seen from Figure 4A, the absorption observed in experiments using half and full dose was less than expected from a linear extrapolation of the low dose data. This observation suggests that unwanted radical−radical reactions such as reactions 5 and 13 become important at high radical concentrations.

The line through the experimental data in Figure 4A is a linear least-squares fit to the low dose data and has a slope of 0.456 ± 0.038. Combining this slope with the F atom yield of (3.18 ± 0.32) × 10^{15} cm^{-3} (full dose and $[SF_6] = 1000$ mbar[4]), we obtain $\sigma_{250\ nm}((CH_3O)_2CHOCH_2(\cdot)) = (2.77 \pm 0.36) \times 10^{-18}$ cm^2 molecule^{-1}. The quoted uncertainty includes both statistical and potential systematic uncertainties and so reflects the accuracy of the measurement.

The spectrum of the alkyl radical was recorded following the pulsed radiolysis of $SF_6/(CH_3O)_3CH$ mixtures using a diode array camera. The delay was 0.3 μs, the integration time was 0.45 μs, and the spectral resolution was 1 nm. The spectrum

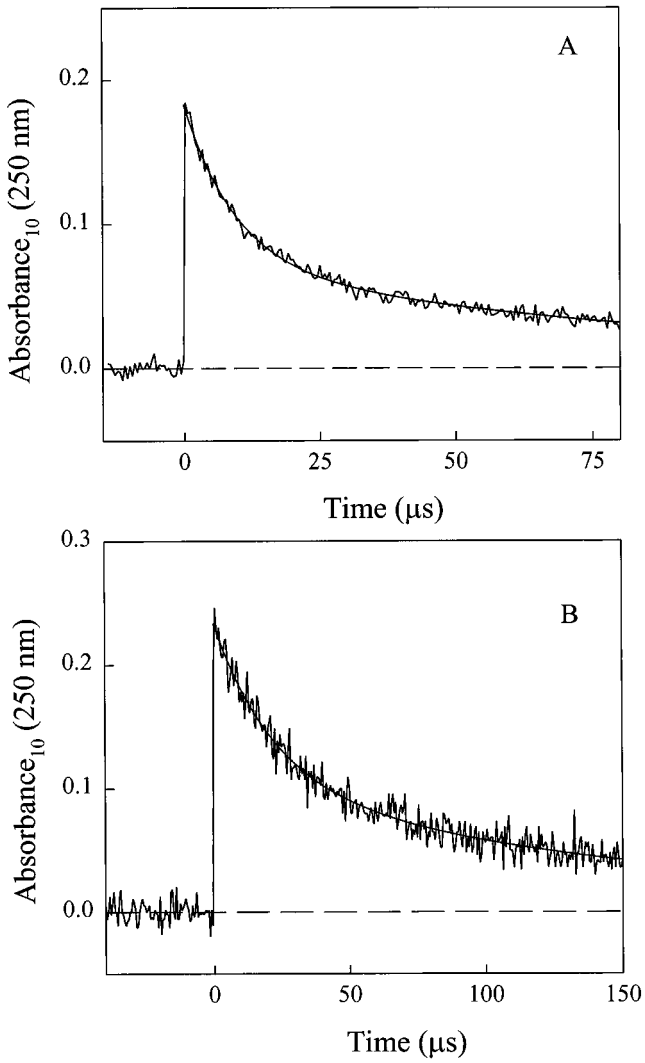

Figure 3. Transient absorption at 250 nm following the pulsed radiolysis of mixtures of (A) 5 mbar $(CH_3O)_3CH$ and 995 mbar SF_6, and (B) 5 mbar $(CH_3O)_3CH$, 20 mbar O_2, and 975 mbar SF_6.

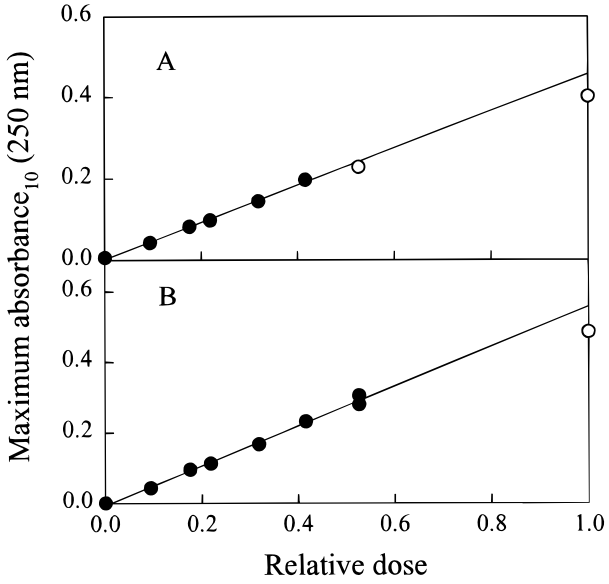

Figure 4. Maximum transient absorbance at 250 nm versus radiolysis dose using mixtures of (A) 5 mbar $(CH_3O)_3CH$ and 995 mbar SF_6, and (B) 5 mbar$(CH_3O)_3CH$, 20 mbar O_2, and 995 mbar SF_6. The solid lines are linear regressions of the low dose data (filled circles). The optical path length was 120 cm.

TABLE 1: Absorption Cross Sections Measured in This Work

wavelength (nm)	$\sigma((CH_3O)_2CHOCH_2(\cdot)$ (10^{-20} cm^2 molecule^{-1})	$\sigma((CH_3O)_2CHOCH_2O_2(\cdot)$ (10^{-20} cm^2 molecule^{-1})
220	385	390
230	319	409
240	274	388
250	277	351
260	294	271
270	294	169
280	278	96
290	234	61
300	160	37
310	104	30
320	58	32

was placed on an absolute basis using $\sigma_{250\ nm} = 2.77 \times 10^{-18}$ cm^2 molecule^{-1} to give the results shown in Table 1 and Figure 5A. For comparison the UV absorption spectrum of the $CH_3OCH_2(\cdot)$ radical[10] is also given in Figure 5A. As with the $(CH_3O)_2CHOCH_2(\cdot)$ radical, the spectrum of the $CH_3OCH_2(\cdot)$ radical has two absorption bands in the 220−320 nm region.

In the analysis above we have assumed that F atoms react with trimethoxymethane to give $(CH_3O)_2CHOCH_2(\cdot)$ radicals. As discussed in section 3.2, the reaction of F atoms with trimethoxymethane proceeds at a rate close to the gas kinetic limit. The relative importance of H atom abstraction from the two possible sites in trimethoxymethane is expected to be proportional to the number of different C−H bonds. Hence, the spectrum labeled as "$(CH_3O)_2C(H)OCH_2(\cdot)$" in Figure 5A is in reality a composite spectrum consisting of 90% $(CH_3O)_2C(H)OCH_2(\cdot)$ and 10% $(CH_3O)_3C(\cdot)$ radicals. At the present time we are unable to separate the contribution of the two radical species. Based upon the database for similar alkyl radicals, the UV spectra of the two different radicals are not expected to be grossly different and it seems reasonable to proceed on the assumption that the spectrum given in Figure 5A is close to, or indistinguishable from, that of "pure" $(CH_3O)_2C(H)OCH_2(\cdot)$ radicals. Analogous assumptions are made in sections 3.4−3.9 and are not discussed further.

3.4. Kinetic Study of the Self-Reaction of $(CH_3O)_2CHOCH_2(\cdot)$ Radicals. Figure 3A shows a typical absorption transient obtained by pulse radiolysis of a mixture of 995 mbar of SF_6 and 5 mbar of $(CH_3O)_3CH$. The transient shows a rapid increase in absorption at 250 nm followed by a slower decay. We ascribe the decay to the self-reaction of the $(CH_3O)_2CHOCH_2(\cdot)$ alkyl radical, via reaction 5:

$$(CH_3O)_2CHOCH_2(\cdot) + (CH_3O)_2CHOCH_2(\cdot) \rightarrow \text{products} \quad (5)$$

The decay follows second-order kinetics and was fitted with the second-order decay expression $A(t) = (A_0 - A_{inf})/(1 + 2k(A_0 - A_{inf})t) + A_{inf}$, where $A(t)$ is the measured absorbance at time t, and A_0 and A_{inf} are the absorbances extrapolated to time zero and infinite time, respectively. The smooth curve in Figure 3A is a second-order fit. No residual absorption was observed, indicating the absence of any product(s) which absorb at 250 nm.

The reciprocal half-lives, $1/t_{1/2}$ (derived from the fits), are plotted as a function of A_0 in Figure 6 (circles). The $(CH_3O)_2CHOCH_2(\cdot)$ alkyl radical concentration and hence A_0 was varied by changing the radiolysis dose and hence initial F atom concentration. A linear least-squares fit of the circles in Figure 6 gives a slope of $(4.91 \pm 0.10) \times 10^5\ s^{-1} = (k_5 \times 2 \ln 10)/(\sigma(\text{alkyl})L)$, where σ(alkyl) is the absorption cross section of

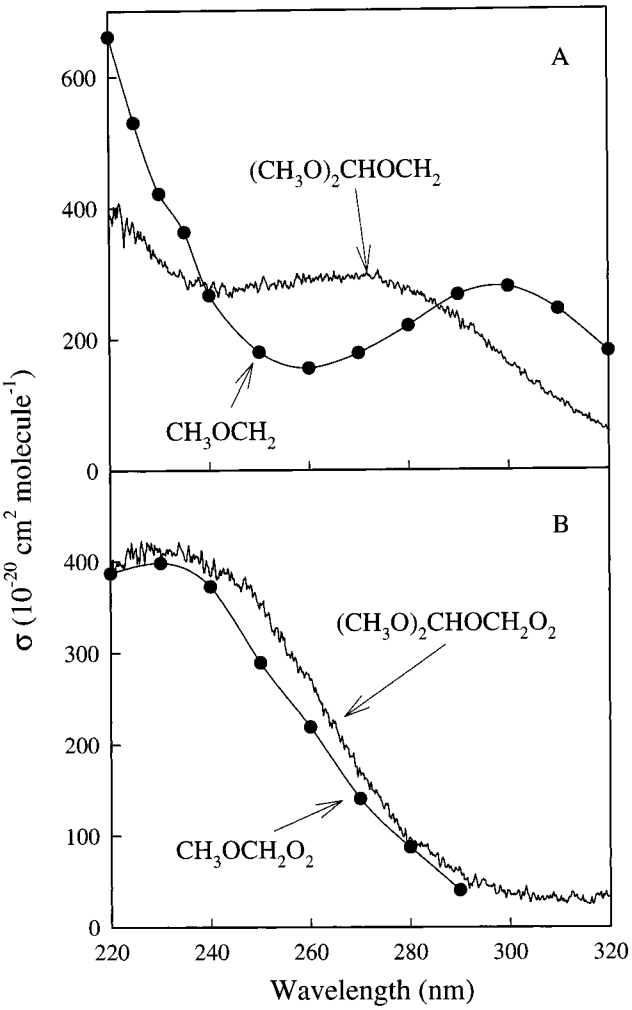

Figure 5. (A) UV-absorption spectra of $(CH_3O)_2CHOCH_2(\cdot)$ (this work) and $CH_3OCH_2(\cdot)$.[10] (B) UV-absorption spectra of $(CH_3O)_2CHOCH_2O_2(\cdot)$ and $CH_3OCH_2O_2(\cdot)$.[13]

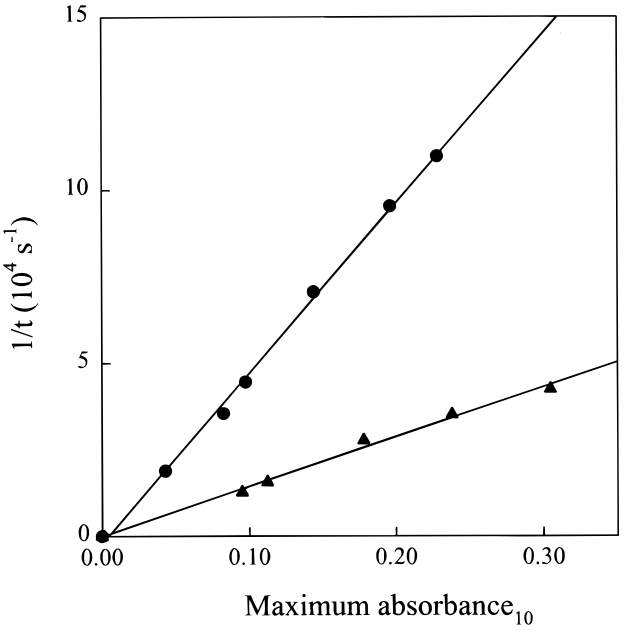

Figure 6. Reciprocal half-life for the self-reaction of the $(CH_3O)_2CHOCH_2(\cdot)$ (circles) and $(CH_3O)_2CHOCH_2O_2(\cdot)$ (triangles) radicals as a function of maximum absorbance at 250 nm.

the $(CH_3O)_2CHOCH_2(\cdot)$ alkyl radical at 250 nm, and L is the optical path length (120 cm). Hence, we derive $k_5 = (3.54 \pm 0.47) \times 10^{-11}$ cm^3 molecule^{-1} s^{-1}. The quoted error includes statistical uncertainties in both the slope in Figure 6 and the absorption cross section of the $(CH_3O)_2CHOCH_2(\cdot)$ radical. The magnitude of k_5 is similar to the rate constants reported for the self-reaction of CH_3OCH_2 alkyl radicals, $(4.1 \pm 0.5) \times 10^{-11}$ cm^3 molecule^{-1} s^{-1}.[11]

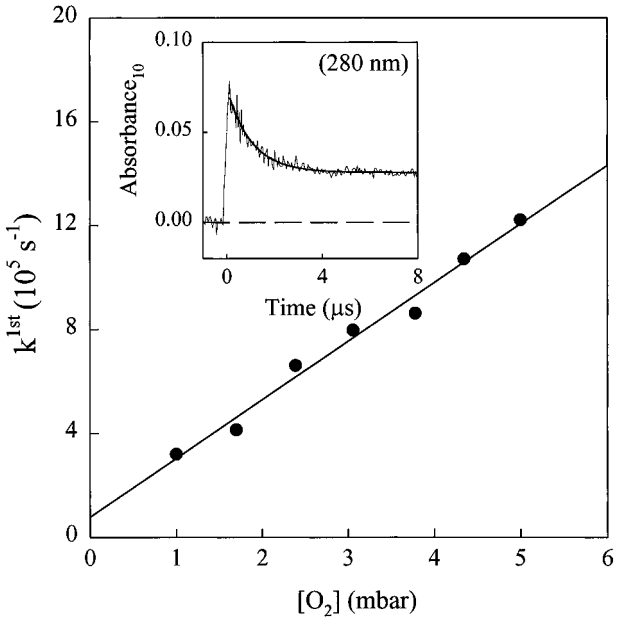

Figure 7. Pseudo-first-order rate constants for the formation of $(CH_3O)_2CHOCH_2O_2(\cdot)$ radicals as a function of the O_2 concentration in 1000 mbar of SF_6, diluent, measured at 280 nm. The insert shows an experimental transient obtained using a mixture of 3.18 mbar $(CH_3O)_3CH$, 4.35 mbar of O_2, in 992.5 mbar of SF_6. The UV path length was 120 cm, and the radiolysis dose was 22% of maximum.

3.5. Association Reaction between O_2 and the $(CH_3O)_2CHOCH_2(\cdot)$ Radical. The kinetics of reaction 2 were studied by monitoring the absorbance at 280 nm following pulse radiolysis mixtures of 992−996 mbar of SF_6, 3.0 mbar of $(CH_3O)_3CH$, and 1.1−5.0 mbar of O_2.

$$(CH_3O)_2CHOCH_2(\cdot) + O_2 + M \rightarrow (CH_3O)_2CHOCH_2O_2(\cdot) + M \quad (2)$$

Using $k_3 = (3.0 \pm 0.7) \times 10^{-10}$ cm^3 molecule^{-1} s^{-1} it follows that in the presence of 3 mbar of $(CH_3O)_3CH$ the lifetime of F atoms with respect to conversion into $(CH_3O)_2CHOCH_2(\cdot)$ radicals is 0.05 μs. Assuming that $(CH_3O)_2CHOCH_2(\cdot)$ radicals behave like other alkyl radicals and add O_2 with a rate constant of the order $10^{-12}-10^{-11}$ cm^3 molecule^{-1} s^{-1}, the lifetime of $(CH_3O)_2CHOCH_2(\cdot)$ radicals with respect to conversion into $(CH_3O)_2CHOCH_2O_2(\cdot)$ radicals will be of the order of a microsecond. Consistent with expectations, the pulsed radiolysis of $SF_6/(CH_3O)_3CH/O_2$ mixtures produced absorption transients which consisted of an initial rapid increase in absorption (complete within 0.2 μs) followed by a rapid decay which occurred on a time scale of 1−2 μs and followed first-order kinetics. The insert in Figure 7 shows a typical absorption transient and a first-order fit. As seen from Figure 7, the pseudo-first-order rate for decay of absorption at 280 nm, k^{first}, increased linearly with the O_2 concentration. It seems reasonable to ascribe the decay of absorption to loss of $(CH_3O)_2CHOCH_2(\cdot)$ radicals via reaction with O_2. Linear least-squares analysis of the data in Figure 7 gives $k_2 = (9.2 \pm 1.5) \times 10^{-12}$ cm^3 molecule^{-1} s^{-1}. The y-axis intercept is $(0.8 \pm 0.9) \times 10^5$ s^{-1} and is not significant. The magnitude of k_2 is typical for addition reactions

of O_2 to a alkyl radical which are typically in the range 1×10^{-12} to 1.5×10^{-11} cm^3 molecule^{-1} s^{-1}.[9] The magnitude of k_2 is indistinguishable from the rate constant for the analogous reaction between $CH_3OCH_2(\cdot)$ radicals and O_2, $(1.09 \pm 0.03) \times 10^{-11}$ cm^3 molecule^{-1} s^{-1}.[11]

3.6. Spectrum of $(CH_3O)_2CHOCH_2O_2(\cdot)$ Radicals. Following the pulse radiolysis of mixtures of 975 mbar SF_6, 5 mbar $(CH_3O)_3CH$, and 20 mbar O_2, a rapid increase (complete within 0.5−2.0 μs) in the UV absorbance was observed, followed by a slower decay. An example is shown in Figure 3B. We ascribe this UV absorbance to the formation of alkyl peroxy radicals via reaction 2. To work under conditions where a known fraction of the F atoms are converted into alkyl peroxy radicals, it is necessary to consider potential complications caused by unwanted radical−radical reactions such as reactions 5, 13, 14, and 15.

$$(CH_3O)_2CHOCH_2(\cdot) + (CH_3O)_2CHOCH_2(\cdot) \rightarrow \text{products} \quad (5)$$

$$F + (CH_3O)_2CHOCH_2(\cdot) \rightarrow \text{products} \quad (13)$$

$$F + (CH_3O)_2CHOCH_2O_2(\cdot) \rightarrow \text{products} \quad (14)$$

$$(CH_3O)_2CHOCH_2(\cdot) + (CH_3O)_2CHOCH_2O_2(\cdot) \rightarrow \text{products} \quad (15)$$

and loss of F atoms by reaction with molecular oxygen, reaction 16:

$$F + O_2 + M \rightarrow FO_2 + M \quad (16)$$

In section 3.2 we report $k_3 = (3.0 \pm 0.7) \times 10^{-10}$; combining this result with $k_{16} = (1.9 \pm 0.3) \times 10^{-13}$ cm^3 molecule^{-1} s^{-1},[12] we calculate that 0.3% of the F atoms are converted into FO_2 radicals and 99.7% into alkyl peroxy radicals. No corrections are necessary for the presence of FO_2 radicals.

There are no literature data concerning the kinetics of reactions 13, 14, and 15, hence we cannot calculate their importance. To check for these unwanted radical−radical reactions, the transient absorbance at 250 nm was measured using mixtures of 975 mbar SF_6, 5 mbar $(CH_3O)_3CH$, and 20 mbar O_2 with the radiolysis dose varied over an order of magnitude. The UV path length was 120 cm. Figure 4B shows the observed maximum absorbance of the experimental transients at 250 nm as a function of dose. As seen from Figure 4B, at full dose the transient absorbance falls below that expected from a linear extrapolation of the low dose data. We ascribe this to incomplete conversion of F atoms into alkyl peroxy radicals caused by secondary radical−radical reactions 5, 13, 14, and 15 at high radical concentrations. The solid line drawn through the data in Figure 4B is a linear least-squares fit of the low dose data. The slope is 0.56 ± 0.03. From this value and the yield of F atoms of $(3.18 \pm 0.32) \times 10^{15}$ cm^{-3} (full dose and $[SF_6] = 1000$ mbar[4]) we derive $\sigma_{250\ nm}$ $(CH_3O)_2CHOCH_2O_2(\cdot) = (3.51 \pm 0.40) \times 10^{-18}$ cm^2 molecule^{-1}. The quoted uncertainty includes both statistical and potential systematic uncertainties and so reflects the accuracy of the measurement.

The UV spectrum of the alkyl peroxy radical was recorded using a diode array camera following the pulsed radiolysis of $SF_6/(CH_3O)_3CH/O_2$ mixtures. The delay was 1.5 μs, the integration time was 0.75 μs, and the spectral resolution was 1 nm. The spectrum was placed on an absolute basis using $\sigma_{250\ nm}$ $(CH_3O)_2CHOCH_2O_2(\cdot) = 3.51 \times 10^{-18}$ cm^2 molecule^{-1}. The result is shown in Figure 5B, and selected cross sections are given in Table 1. For comparison the UV spectrum of the $CH_3OCH_2O_2(\cdot)$ radical is also given in Figure 5B. As expected for such similar radicals the two spectra are indistinguishable. The UV absorption spectra of alkyl peroxy radicals typically consist of a broad featureless band in the region 200−300 nm with a maximum absorption cross section at ≈ 240−250 nm of $(4-5) \times 10^{-18}$ cm^2 molecule^{-1}.[13] Inspection of Figure 5B shows that the UV spectra of $CH_3OCH_2O_2(\cdot)$ and $(CH_3O)_2CHOCH_2O_2(\cdot)$ radicals are typical for this class of radical species.

3.7. Kinetic Study of the Self-Reaction of $(CH_3O)_2CHOCH_2O_2(\cdot)$ Radicals. Following the pulse radiolysis of $SF_6/(CH_3O)_3CH/O_2$ mixtures a rapid increase in the absorbance at 250 nm was observed followed by a slower decay (see Figure 3B). We ascribe the decay of the absorption to loss of alkyl peroxy radicals via reaction 6:

$$(CH_3O)_2CHOCH_2O_2(\cdot) + (CH_3O)_2CHOCH_2O_2(\cdot) \rightarrow \text{products} \quad (6)$$

The decay followed second-order decay kinetics and was fitted with the expression $A(t) = (A_0 - A_{inf})/(1 + 2k_{6\ obs}(A_0 - A_{inf})t) + A_{inf}$; where $A(t)$ is the measured absorbance at time t, A_0 is the absorbance at time zero, A_{inf} is the absorbance at infinite time, and $k_{6\ obs}$ is the observed second-order rate constant for reaction 6. From the fit, the half-life ($t_{1/2}$) for the self-reaction was calculated. Experiments were performed using mixtures of 975 mbar SF_6, 5 mbar $(CH_3O)_3CH$, and 20 mbar O_2. The initial alkyl peroxy radical concentration was varied by varying the radiolysis dose. The triangles in Figure 6 shows the reciprocal half-lives ($1/t_{1/2}$) plotted as a function of A_0, where A_0 is the absorbance of the alkyl peroxy radical at $t = 0$. A linear least-squares fit gives a slope of $(1.44 \pm 0.06) \times 10^5$ s^{-1} $= (k_{5\ obs} \times 2\ \ln\ 10)/(\sigma_{alkyl\ peroxy} \times L)$, where $\sigma_{alkyl\ peroxy}$ is the absorption cross section of the $(CH_3O)_2CHOCH_2O_2(\cdot)$ radical, and L is the optical path length (120 cm). Hence, we derive $k_{5\ obs} = (1.31 \pm 0.16) \times 10^{-11}$ cm^3 molecule^{-1} s^{-1}. The quoted error includes statistical uncertainties from analysis of the data in Figure 6 and the absorption cross section of the $(CH_3O)_2CHOCH_2O_2(\cdot)$ radical.

3.8. Kinetics of the Reaction between $(CH_3O)_2CHOCH_2O_2(\cdot)$ Radicals and NO. The kinetics of reaction 7 were studied by monitoring the increase in absorbance at 400 nm due to NO_2 formation following the radiolysis of mixtures of 5 mbar $(CH_3O)_3CH$, 20 mbar O_2, 0.11−0.94 mbar NO in 1000 mbar of SF_6 diluent. The insert in Figure 8A shows the absorbance as a function of time after the pulsed radiolysis of a mixture containing 0.65 mbar of NO. NO_2 absorbs strongly at 400 nm and we ascribe the increase in absorbance to NO_2 formation via reaction 7a.

$$(CH_3O)_2CHOCH_2O_2(\cdot) + NO \rightarrow (CH_3O)_2CHOCH_2O + NO_2 \quad (7a)$$

$$(CH_3O)_2CHOCH_2O_2(\cdot) + NO + M \rightarrow (CH_3O)_2CHOCH_2ONO_2 + M \quad (7b)$$

For each concentration of NO the increase in absorption was fitted using the following expression for a first order formation: $A(t) = (A_{inf} - A_0)(1 - \exp(-k^{first}t)) + A_0$, where $A(t)$ is the time-dependent absorbance, A_0 is the absorbance at time $t = 0$ (always close to zero), A_{inf} is the absorbance at infinite time, and k^{first} is the pseudo-first-order appearance rate of NO_2. As seen from Figure 8A, the pseudo-first-order rate constants increased linearly with the NO concentration. Linear least-

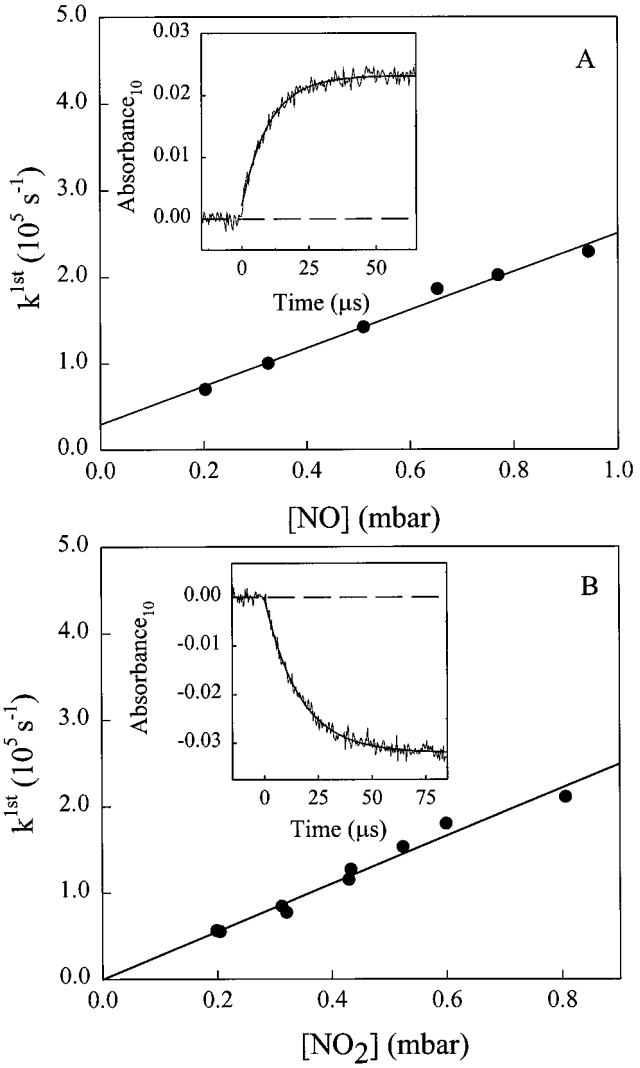

Figure 8. (A) Plot of the pseudo-first-order rate constant for NO_2 formation as a function of the NO concentration. (B) Plot of the pseudo-first-order rate constant for NO_2 loss versus the NO_2 concentration. The inserts show typical absorption transients at 400 nm following radiolysis (dose = 22% of maximum) of mixtures of 5 mbar $(CH_3O)_3CH$, 20 mbar O_2, 975 mbar SF_6, and either 0.65 mbar NO (A) or 0.33 NO_2 (B).

squares analysis of the data in Figure 8A gives $k_7 = (9.0 \pm 1.2) \times 10^{-12}$ cm^3 molecule^{-1} s^{-1}. The *y*-axis intercept is $(2.9 \pm 1.6) \times 10^4$ s^{-1} and suggests that self-reaction contributes to the loss of peroxy radicals. The decay half-life for the loss of $(CH_3O)_2CHOCH_2O_2(\cdot)$ due to the self-reaction is approximately 22 μs at 22% of maximum dose. An intercept of 2.9×10^4 s^{-1} which is the same as a first-order formation half-life for NO_2 of 34 μs is close to the decay half-life for $(CH_3O)_2CHOCH_2O_2(\cdot)$ due to the self-reaction. Hence, on a semiquantitative basis the intercept in Figure 8A can be explained by the self-reaction of $(CH_3O)_2CHOCH_2O_2(\cdot)$ radicals. To test this hypothesis, the experimental transient shown in Figure 8A was simulated using a model consisting of the following reactions (and rate constants): F + RH (3.0×10^{-10}), R + O_2 (9.2×10^{-12}), R + R (3.5×10^{-11}), RO_2 + RO_2 (1.31×10^{-11}), RO_2 + NO (9.0×10^{-12}), RO + NO(1×10^{-11}), RO + NO_2 (1×10^{-11}), RO_2 + NO_2 (1.0×10^{-11}) with $\sigma(NO_2) = 6.01 \times 10^{-19}$ cm^2 molecule^{-1} at 400 nm. The resulting simulated transient was indistinguishable from the first-order fit shown in Figure 8A.

3.9. Kinetics of the Reaction between $(CH_3O)_2CHOCH_2O_2(\cdot)$ Radicals and NO_2. The kinetics of reaction 8 were studied by monitoring the decrease in absorbance at 400 nm following the pulsed radiolysis of mixtures of 5 mbar $(CH_3O)_3CH$, 20 mbar O_2, 0.13−0.82 mbar NO_2, in 1000 mbar total pressure of SF_6 diluent. The insert in Figure 8A shows the absorbance as a function of time after the radiolysis of a mixture containing 0.35 mbar of NO_2. The rate of decay of the absorbance at 400 nm increased linearly with the NO_2 concentration. It seems reasonable to ascribe the loss of absorbance to loss of NO_2 in the system. Three reactions could be responsible for the NO_2 loss:

$$F + NO_2 + M \rightarrow FNO_2/FONO + M \quad (17)$$

$$(CH_3O)_2CHOCH_2(\cdot) + NO_2 \rightarrow \text{products} \quad (18)$$

$$(CH_3O)_2CHOCH_2O_2(\cdot) + NO_2 + M \rightarrow (CH_3O)_2CHOCH_2O_2NO_2 + M \quad (8)$$

However, the time scale of the decay shown in the insert in Figure 8A is only consistent with reaction 8 causing the loss of NO_2 (the lifetimes for both F atoms and $(CH_3O)_2CHOCH_2(\cdot)$ radicals are <0.1 μs, see sections 3.2 and 3.5). The smooth curve in Figure 8B is a first-order fit which gives a pseudo-first-order rate constant, k^{first}, = 8.44×10^4 s^{-1}. To allow sufficient time for conversion of F atoms into the alkyl peroxy radicals the analysis of the decay traces was performed starting 2 μs after the radiolysis pulse. k^{first} values for 10 experiments with different concentrations of NO_2 are shown in Figure 8B. Linear least-squares analysis of the data in Figure 8B gives $k_8 = (1.00 \pm 0.15) \times 10^{-11}$ cm^3 molecule^{-1} s^{-1}.

3.10. Kinetics of the Reaction of Cl Atoms with $(CH_3O)_3CH$. Prior to investigating the atmospheric fate of the $(CH_3O)_2CHOCH_2(\cdot)$ radical, relative rate experiments were performed using the FTIR system to investigate the kinetics of the reactions of Cl atoms with $(CH_3O)_3CH$. The techniques are described in detail elsewhere.[14] Photolysis of molecular chlorine was the source of Cl atoms.

$$Cl_2 \xrightarrow{h\nu} 2Cl \quad (19)$$

$$Cl + (CH_3O)_3CH \rightarrow \text{products} \quad (20)$$

The kinetics of reaction 20 were measured relative to reactions 21 and 22.

$$Cl + C_2H_4 \rightarrow \text{products} \quad (21)$$

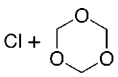

(22)

In relative rate studies it is important to establish that the reactant and reference compounds are lost solely via the reaction of interest. To check for heterogeneous loss of $(CH_3O)_3CH$ in the chamber 10.3 mTorr of this compound was introduced in 700 Torr of air and allowed to stand in the dark for 5 min. A small (0.62 mTorr) but significant loss of $(CH_3O)_3CH$ was observed, and 0.69 mTorr of methyl formate and 1.19 mTorr of CH_3OH were formed. On repeating this control experiment the loss of $(CH_3O)_3CH$ was less pronounced (3% in 10 min) consistent with a conditioning of the chamber walls for this species. On the basis of the moisture sensitivity of $(CH_3O)_3CH$[15] and the observed formation of methyl formate and CH_3OH in molar yields consistent with hydrolysis we believe that the loss of $(CH_3O)_3CH$ is attributable to hydrolysis with water on the chamber walls. To minimize potential complications

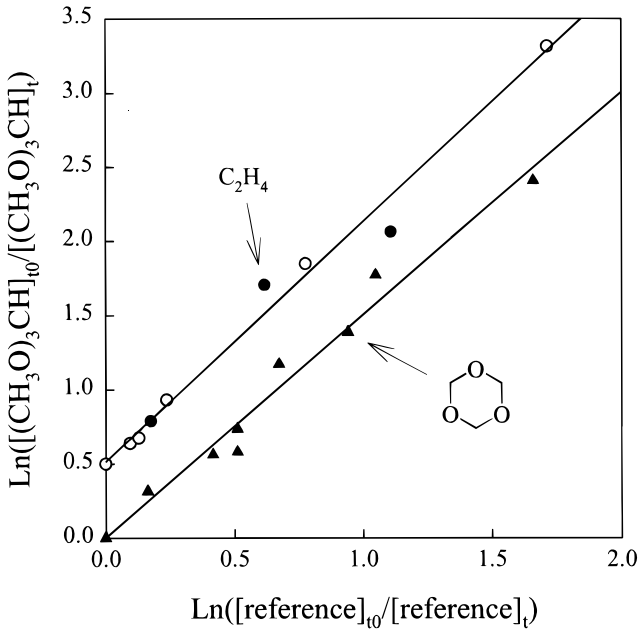

Figure 9. Decay of $(CH_3O)_3CH$ versus C_2H_4 and 1,3,5-trioxane when mixtures of these compounds were exposed to Cl atoms in 700 Torr of air (filled symbols) or N_2 (open symbols). For clarity the data using C_2H_4 reference have been shifted vertically by 0.5 units.

caused by such hydrolysis, the chamber was "dried" by exposure to air/$(CH_3O)_3CH$ mixtures prior to the start of each set of experiments. The observed loss of $(CH_3O)_3CH$ versus that of the reference compounds following the UV irradiation of $(CH_3O)_3CH$/reference/Cl_2 mixtures in 700 Torr total pressure of N_2, or air, diluent is shown in Figure 9. A small (2%) correction has been applied to the loss of $(CH_3O)_3CH$ to account for loss via hydrolysis (as measured by the formation of methyl formate) during the experiments. There was no discernible difference between data obtained using N_2 or air diluent. For clarity the data using C_2H_4 reference have been shifted vertically by 0.5 units. Linear least-squares analysis of the data shown in Figure 9 gives $k_{20}/k_{21} = 1.62 \pm 0.11$ and $k_{20}/k_{22} = 1.50 \pm 0.15$. Using $k_{21} = 9.4 \times 10^{-11}$ [16] and $k_{22} = 1.03 \times 10^{-10}$ cm^3 molecule^{-1} s^{-1},[17] gives $k_{20} = (1.52 \pm 0.10) \times 10^{-10}$, and $k_{20} = (1.54 \pm 0.15) \times 10^{-10}$ cm^3 molecule^{-1} s^{-1}. Consistent results were obtained using the different reference compounds. We choose to quote a value for k_{20} which is the average of the results above with error limits which encompass the extremes of the ranges, hence $k_{20} = (1.53 \pm 0.16) \times 10^{-10}$ cm^3 molecule^{-1} s^{-1}. We estimate that potential systematic errors associated with uncertainties in the reference rate constants could add an additional 10% uncertainty. Propagating this additional 10% uncertainty gives $k_{20} = (1.53 \pm 0.22) \times 10^{-10}$ cm^3 molecule^{-1} s^{-1}. There are no literature data to compare with this result.

3.11. Atmospheric Fate of Alkyl Radicals Derived from $(CH_3O)_3CH$. When trimethoxymethane is oxidized in the atmosphere, two different alkyl radicals are formed depending on the site of OH reaction; $(CH_3O)_3C(\cdot)$ and $(CH_3O)_2C(H)OCH_2(\cdot)$. As shown in section 3.5 these alkyl radicals add O_2 with a rate constant of approximately 1×10^{-11} cm^3 molecule^{-1} s^{-1}. In one atmosphere of air the lifetime of the $(CH_3O)_3C(\cdot)$ and $(CH_3O)_2C(H)OCH_2(\cdot)$ radicals with respect to addition of O_2 will be approximately 20 ns. Decomposition via reaction 23 is a possible competing fate of $(CH_3O)_2C(H)OCH_2(\cdot)$ radicals which needs consideration:

$$(CH_3O)_2C(H)OCH_2(\cdot) + M \rightarrow (CH_3O)_2CH(\cdot) + HCHO + M \quad (23)$$

To test for the potential importance of reaction 23 experiments were performed using mixtures of 7 mTorr of $(CH_3O)_3CH$ and 111 mTorr of Cl_2 in 700 Torr of N_2. In such experiments there is a competition between reactions 23 and 24 for the available $(CH_3O)_2C(H)OCH_2(\cdot)$ radicals:

$$(CH_3O)_2C(H)OCH_2(\cdot) + Cl_2 \rightarrow (CH_3O)_2C(H)OCH_2Cl + Cl \quad (24)$$

There was no observable HCHO formation (<3% molar yield) following UV irradiation of $(CH_3O)_3CH/Cl_2/N_2$ mixtures and we conclude that loss of $(CH_3O)_2C(H)OCH_2(\cdot)$ radicals via reaction 23 is of no significance. Alkyl radicals typically react with O_2 and Cl_2 with rate constants which are of a similar magnitude,[9] and we conclude that reaction 23 is of no importance in the atmospheric chemistry of $(CH_3O)_2C(H)OCH_2(\cdot)$ radicals.

3.12. Atmospheric Fate of Alkoxy Radicals Derived from $(CH_3O)_3CH$. The peroxy radicals formed during the atmospheric oxidation of trimethoxymethane will react with NO to give two different alkoxy radicals: $(CH_3O)_3CO(\cdot)$ and $(CH_3O)_2C(H)OCH_2O(\cdot)$. The tertiary alkoxy radical is expected to eliminate a $CH_3O(\cdot)$ radical to give dimethyl carbonate (DMC).

$$(CH_3O)_3CO(\cdot) + M \rightarrow (CH_3O)_2CO\ (DMC) + CH_3O(\cdot) \quad (25)$$

The primary alkoxy radical has several possible fates:

$$(CH_3O)_2C(H)OCH_2O(\cdot) + M \rightarrow (CH_3O)_2CHOC(O)H + H + M \quad (26)$$

$$(CH_3O)_2C(H)OCH_2O(\cdot) + M \rightarrow (CH_3O)_2C(H)O(\cdot) + HCHO + M \quad (27)$$

$$(CH_3O)_2C(H)OCH_2O(\cdot) \rightarrow CH_3OC(H)(OCH_2OH)OCH_2(\cdot) \quad (28)$$

$$(CH_3O)_2C(H)OCH_2O(\cdot) + O_2 \rightarrow (CH_3O)_2CHOC(O)H + HO_2 \quad (29)$$

To provide insight into the relative importance of reactions 26−29 a product study of the OH radical-initiated oxidation of trimethoxymethane in 700 Torr of air diluent was undertaken using mixtures of 14.2 mTorr of trimethoxymethane, 90 mTorr of CH_3ONO, and 6 mTorr of NO in 700 Torr of air diluent. Dimethyl carbonate (DMC) was identified using its characteristic IR spectrum[4] as the major product. After correcting the observed loss of trimethoxymethane for the formation of a significant (30%) yield of methyl formate attributable to hydrolysis of trimethoxymethane (see section 3.11), it was determined that the OH-initiated oxidation of trimethoxymethane produces dimethyl carbonate in a molar yield of 81 ± 10%. The fate of the remaining 19% of the trimethoxymethane is unknown. As noted above, the OH radical-initiated atmospheric oxidation of trimethoxymethane produces two different alkoxy radicals. The relative yields of these two alkoxy radicals is dictated by the relative rates of attack of OH radicals on the two different C−H bonds in trimethoxymethane. OH radicals react with CH_3OCH_3, $CH_3OCH_2OCH_3$, and $(CH_3O)_4C$ via H-atom abstraction with rate constants of 2.9×10^{-12},[18] 5.2×10^{-12},[6,7] and 4.7×10^{-12} [19] cm^3 molecule^{-1} s^{-1}, respectively, and 76% of the attack

occurs on the $-CH_3$ end groups in $CH_3OCH_2OCH_3$.[6] OH radical attack on the $-OCH_3$ groups in CH_3OCH_3, $CH_3OCH_2OCH_3$, and $(CH_3O)_4C$ occurs with rate constants of 1.5×10^{-12}, 2.0×10^{-12}, and 1.2×10^{-12} cm^3 molecule^{-1} s^{-1}. The reactivity of the individual $-OCH_3$ groups in CH_3OCH_3, $CH_3OCH_2OCH_3$, and $(CH_3O)_4C$ are similar. It seems reasonable to assume that the reactivity of an individual $-OCH_3$ group in trimethoxymethane will be close to the average observed in CH_3OCH_3, $CH_3OCH_2OCH_3$, and $(CH_3O)_4C$. Hence, we estimate that approximately 80% of reaction 1 proceeds via attack on the $-OCH_3$ groups and we conclude that the observed dimethyl carbonate product is largely associated with chemistry involving the $(CH_3O)_2C(H)OCH_2O(\cdot)$ radical. Of the four possible fates of the $(CH_3O)_2C(H)OCH_2O(\cdot)$, only reaction 27 followed by reaction 30 can account for the observed DMC yield and we conclude that reaction 27 is the major atmospheric fate of $(CH_3O)_2C(H)OCH_2O(\cdot)$ radicals.

$$(CH_3O)_2C(H)O(\cdot) + O_2 \rightarrow (CH_3O)_2CO\ (DMC) + HO_2(\cdot) \quad (30)$$

Discussion

A substantial body of kinetic and mechanistic data pertaining to the atmospheric chemistry of trimethoxymethane is presented here. At 296 K, the rate constant for reaction of OH radicals with dimethoxymethane is 6.0×10^{-12} cm^3 molecule^{-1} s^{-1}. While the OH radical concentration in the atmosphere varies with location, time of day, season, and meteorological conditions, a reasonable global 24 h global average is $(0.5-1.0) \times 10^6$ cm^{-3}.[20-22] Hence, the atmospheric lifetime of trimethoxymethane with respect to reaction with OH radicals is 2−4 days. As noted in section 3.10, surface-catalyzed hydrolysis of trimethoxymethane proceeds rapidly and is likely to be an important atmospheric loss mechanism. Dimethyl carbonate is the major product of the OH radical-initiated oxidation of trimethoxymethane. As discussed elsewhere,[4] dimethyl carbonate is a relatively unreactive compound with an atmospheric lifetime of approximately two months. The modest reactivity of trimethoxymethane toward OH radicals combined with its formation of oxidation products which are essentially unreactive gives trimethoxymethane a low ozone-forming potential in urban air masses.

It is interesting to compare the measured reactivity of OH radicals with trimethoxymethane with estimations using the structure activity relationship (SAR) approach developed by Atkinson and co-workers.[23,24] The SAR method estimates rate constants for reactions of OH radicals with organic compounds by assuming that the reactivity of each part of the molecule is separate and influenced only by its nearest neighbors. A strict application of the SAR method to trimethoxymethane gives a value for k_1 which is greater than the gas kinetic limit and is not physically reasonable; $k_1 = 3k_{prim}F(-OR) + k_{tert}[F(-OR)]^3 = 1.1 \times 10^{-9}$ cm^3 molecule^{-1} s^{-1}. As noted previously,[24] rigid application of the SAR technique grossly overestimates the reactivity of polyethers and better agreement is achieved if only one α substituent factor is used which then gives $k_1 = 3k_{prim}F(-OR) + k_{tert}[F(-OR)] = 2.0 \times 10^{-11}$ cm^3 molecule^{-1} s^{-1}; a factor of 3 greater than that measured herein. SAR methods have limited utility in predicting the reactivity of polyethers.

References and Notes

(1) Roubi, M. A. *Chem. Eng.* **1995**, *44*, 37.
(2) Hansen, K. B.; Wilbrandt, R.; Pagsberg, P. *Rev. Sci. Instr.* **1979**, *50*, 1532.
(3) Wallington, T. J.; Japar, S. M. *J. Atmos. Chem.* **1989**, *9*, 399.
(4) Bilde, M.; Møgelberg, T. E.; Sehested, J.; Nielsen, O. J.; Wallington, T. J.; Hurley, M. D.; Japar, S. M.; Dill, M.; Orkin, V. L.; Buckley, T. J.; Huie, R. E.; Kurylo, M. J. *J. Phys. Chem. A* **1997**, *101*, 3514.
(5) Nielsen, O. J.; Sidebottom, H. W.; Nelson, L.; Treacy, J. J.; O'Farrel, D. J. *Int. J. Chem. Kinet.* **1989**, *21*, 1101.
(6) Wallington, T. J.; Hurley, M. D.; Ball, J. C.; Straccia, A. M.; Platz, J.; Christensen, L. K.; Sehested, J.; Nielsen, O. J. *J. Phys. Chem. A* **1997**, *101*, 5302.
(7) Porter, E.; Wenger, J.; Treacy, J.; Sidebottom, H., *J. Phys. Chem. A* **1997**, *101*, 5770.
(8) Wallington, T. J.; Hurley, M. D.; Maricq, M. M.; Sehested, J.; Nielsen, O. J.; Ellermann, T. *Int. J. Chem. Kinet.* **1993**, *25*, 651.
(9) Westley, F.; Frizzell, D. H.; Herron, J. T.; Hampson, R. F.; Mallard, W. G. NIST Chemical Kinetics Database Version 6.01, NIST, Gaitherburg, MD, 1994.
(10) Langer, S.; Ljungström, E.; Ellermann, T.; Nielsen, O. J.; Sehested, *J. Chem. Phys. Lett.* **1995**, *240*, 53.
(11) Sehested, J.; Sehested, K.; Platz, J.; Egsgaard, H.; Nielsen, O. J. *Int. J. Chem. Kinet.* **1997**, *29*, 627.
(12) Ellermann, T.; Sehested, J.; Nielsen, O. J.; Pagsberg, P.; Wallington, T. J. *Chem. Phys. Lett.* **1994**, *218*, 287.
(13) Lightfoot, P. D.; Cox, R. A.; Crowley, J. N.; Destriau, M.; Hayman, G. D.; Jenkin, M. E.; Moortgat, G. K.; Zabel, F. *Atmos. Environ.* **1992**, *26*, 1805.
(14) Wallington, T. J.; Hurley, M. D. *Chem. Phys. Lett.* **1992**, *189*, 437
(15) Catalog Handbook of Fine Chemicals, Aldrich Chemical Co., 1997.
(16) DeMore, W. B.; Sander, S. P.; Golden, D. M.; Hampson, R. F.; Kurylo, M. J.; Howard, C. J.; Ravishankara, A. R.; Kolb, C. E.; Molina, M. J. Jet Propulsion Laboratory Publication 97-4, Pasadena, CA, 1997.
(17) Platz, J.; Christensen, L. K.; Sehested, J.; Nielsen, O. J.; Wallington, T. J.; Sauer, C.; Barnes, I.; Becker, K. H.; Vogt, R. *J. Phys. Chem. A* **1998**, *102*, 4829.
(18) Atkinson, R.; Baulch, D. L.; Cox, R. A.; Hampson, R. F.; Kerr, J. A.; Rossi, M. J.; Troe, J. *J. Phys. Chem. Ref. Data* **1997**, *26*, 521.
(19) Platz, J. *unpublished results*.
(20) Ravishankara, A. R.; Lovejoy, E. R. *J. Chem. Soc., Faraday Trans.* **1994**, *90*, 2159.
(21) Dorn, H.-P.; Brandenburger, U.; Brauers, T.; Ehhalt, D. H. *Geophys. Res. Lett.* **1996**, *23*, 2537.
(22) Hofzumahaus, A.; Aschmutat, U.; He*β*ling, M.; Holland, F.; Ehhalt, D. H. *Geophys. Res. Lett.* **1996**, *23*, 2541.
(23) Atkinson, R., *Int. J. Chem. Kinet.* **1987**, *19*, 799.
(24) Atkinson, R.; Kwok, E. S. C. *Atmos. Environ.* **1995**, *29*, 1685.